Biogeosciences Discuss., https://doi.org/10.5194/bg-2018-284
Manuscript under review for journal Biogeosciences
Discussion started: 15 June 2018

Biogeosciences Discussions Open Access EGU

Diapycnal dissolved organic matter supply into the upper Peruvian oxycline

Alexandra N. Loginova[1*], Sören Thomsen[1,2], Marcus Dengler[1], Jan Lüdke[1], Anja Engel[1]

[1]GEOMAR Helmholtz-Centre for Ocean Research Kiel, Düsternbrooker Weg 20, Kiel, 24105, Germany
[2]LOCEAN-IPSL, IRD/CNRS/Sorbonnes Universites (UPMC)/MNHN, Paris, UMR 7159, France
Correspondence to: Anja Engel (aengel@geomar.de)

Abstract. The Eastern Tropical South Pacific (ETSP) hosts the Peruvian upwelling system, which represents one of the most productive areas in the world ocean. High primary production followed by rapid heterotrophic utilization of organic matter supports the formation of one of the most intense oxygen minimum zones (OMZ) in the world ocean where dissolved oxygen (O_2) concentrations reach well below 1 µmol kg^{-1}. The high productivity leads to an accumulation of dissolved organic matter (DOM) in the surface layers that may serve as a substrate for heterotrophic respiration. However, the importance of DOM utilization for O_2 respiration within the Peruvian OMZ remains unclear so far. Here, we evaluate the diapycnal fluxes of O_2, dissolved organic carbon (DOC), dissolved organic nitrogen, dissolved hydrolysable amino acids (DHAA) and dissolved combined carbohydrates (DCCHO) and the composition of DOM in the ETSP off Peru to learn, whether labile DOM is reaching into the core of the OMZ and how important DOM utilization might be for O_2 attenuation. The observed diapycnal O_2 flux (50 mmol O_2 m^{-2} day^{-1} at max) was limited to the upper 80 m of the water column, the flux attenuation of ~1 µmol L^{-1} day^{-1}, was comparable to previously published O_2 consumption rates for the North and South Pacific OMZs. The diapycnal DOM flux (31mmol C m^{-2} day^{-1} at max) was limited to ~30 m water depth, suggesting that the labile DOM is already utilized within the upper part of the shallow oxycline off Peru. The analyses of DCCHO and DHAA composition support this finding, suggesting that DOM undergoes comprehensive remineralization already within the upper part of the oxycline, as the DOM within the core of the OMZ was found to be largely altered. Estimated by a simple equation for carbon combustion, aerobic respiration of DCCHO and DHAA, supplied by diapycnal mixing (0.46 µmol L^{-1} day^{-1} at max), could account for up to 38% of the diapycnal O_2 supply in the upper oxycline, which suggests that DOM utilization may play a significant role for shape of the upper Peruvian oxycline.

1 Introduction

Dissolved oxygen (O_2) plays a key role for biological production and cycling of elements in marine ecosystems as well as for the spatial distribution of marine organisms (Ekau et al., 2010, Gilly et al., 2013). The majority of catabolic processes in organisms are conducted by oxidation with O_2 (e.g. Bender and Heggie 1984). Due to the presence of a pronounced oxygen minimum zone (OMZ) (Karstensen et al., 2008), the eastern tropical South Pacific (ETSP) is one of the largest regions, where the role of O_2 concentrations discriminates. There, O_2 concentrations lower than 1 µmol kg^{-1} are frequently observed between 50 and 400 m depths (Revsbech et al., 2009; Kalvelage et al., 2013; Thomsen et al., 2016a). Those low O_2 concentrations are due to a sluggish ventilation by ocean currents,

Biogeosciences Discuss., https://doi.org/10.5194/bg-2018-284
Manuscript under review for journal Biogeosciences
Discussion started: 15 June 2018

carrying low-O_2 waters to the ETSP and high microbial utilization and to respiration of organic matter (OM) originating from the upper water column (e.g. Czeschel et al., 2011; Brandt et al., 2015; Kalvelage et al., 2015).

Elevated primary production in the Peruvian upwelling region above the OMZ (Pennington et al., 2006) leads to an accumulation of both particulate (POM) (Franz et al., 2012a) and dissolved (DOM) organic matter (Romankevich and Ljutsarev 1990; Franz et al., 2012a; Letscher et al., 2013; Loginova et al., 2016) in the euphotic zone at the continental margin. POM was recognized to be an important source of carbon (C) for microbial OM mineralization (e.g. Dale et al., 2015), utilization of O_2 (Kalvelage et al.,2015), and anoxia-related processes (Kalvelage et al., 2013) in the area. Also, the remineralization of DOM was suggested to contribute significantly to C and O_2 cycling (i.e. Arístegui et al., 2002; Carlson et al., 2011). However, the cycling of DOM in the Peruvian upwelling system has been little studied.

DOM, originating in the euphotic zone, as a result of extracellular release by phytoplankton, cell lysis, particle degradation and sloppy zooplankton feeding (Benner, 2002), is commonly enriched in labile and semi-labile DOM, which are mainly composed of carbohydrates (CHO) and amino acids (AA) (e.g. Ogawa and Tanoue, 2003). Those are preferentially utilized during microbial decomposition of OM, as they serve as energy sources and "building blocks" for microbes to respire and grow (Skoog and Benner, 1997; Lee et al., 2000; Amon et al., 2001). The contribution of CHO and AA to OM, may be used as a measure of OM bioavailability (Davis et al, 2009; Kaiser and Benner, 2009).

Low-O_2 conditions have been suggested to slow down microbial decomposition rates of OM (Harvey et al., 1995; Nguyen and Harvey, 1997). Hence, it could be expected that CHO and AA entering the OMZ would not undergo significant changes. Recent studies in the upwelling area and the corresponding OMZ off Chile, however, found bacterial activity (Leucine-incorporation) of similar range to the oxygenated waters (Sempere et al., 2008, Pantoja et al., 2009). These results suggest that the changes in the remineralization rates of DOM might rather be linked to lack of bioavailable OM supply into the OMZ than to low-O_2 conditions. Herewith, Pantoja et al. (2009) reported relatively high concentrations of free and combined AA in the OMZ off Chile. Sempere et al. (2008) reported lower concentrations of neutral CHO in the corresponding upwelling area, compared to the open Pacific Ocean.

Accessing the possible effects of low-O_2 conditions on the composition of DOM implies that the DOM is transported into the OMZ from the oxygenated waters. Contrary to POM, DOM does not obtain its own gravity flow and its transport is exclusively due to advective and diffusive physical transport processes (e.g. Löscher et al. 2016). In upwelling regimes, turbulent mixing processes are often enhanced near the shelf resulting in high diapycnal fluxes of various solutes (e.g. Schafstall et al., 2010; Kock et al., 2012; Brandt et al., 2015; Steinfeldt et al., 2015). On the other hand, the downward fluxes of DOM, or other solutes, may be reduced or even predominated by upwelling fluxes due to Ekman divergence in the coastal upwelling region (e.g. Steinfeldt et al., 2015).

Machadevan (2014) suggested that transport of OM (via eddy fluxes) into the OMZ should be accompanied by O_2 in amount that is sufficient for full remineralization of the subducted OM. Therefore, this physical transport of OM and O_2 should stimulate heterotrophic aerobic respiration in the OMZ, which was suggested to be the main pathway of OM remineralization in the upper OMZs by Kalvelage et al. (2015). However, so far, no direct O_2 and DOM supply estimates exist for the Peruvian OMZ.

Biogeosciences Discuss., https://doi.org/10.5194/bg-2018-284
Manuscript under review for journal Biogeosciences
Discussion started: 15 June 2018

Using combined physical and biogeochemical observational data, collected during the R/V METEOR "M93" (M93) research cruise to the ETSP off Peru in February-March 2013 we investigate the possible importance of diapycnal DOM supply for the O_2 respiration off Peru. Specifically, we directly estimate the diapycnal O_2 and DOM supply into the upper oxycline off Peru. Additionally, we analyze the composition of dissolved combined CHO and AA to learn, whether DOM and its labile and semi-labile constituents may be supplied to the core of the OMZ.

2 Methods

2.1 Study area

The observational data were acquired during the research cruise "M93" which took place from 7th of February to 9th of March 2013 between 12°S and 14°S and 76°W and 79°W off Peru (Fig.1). During the measurement program, the study area was affected by moderate southeasterly winds (1-9 m/s) (Thomsen et al., 2016a). The water column was highly stratified during the cruise (Fig.2a,b). High concentrations of inorganic nutrients (~30 µmol L^{-1} (NO_3^-), ~3 µmo L^{-1} (PO_4^{3-})) just below the surface (Thomsen et al., 2016a) collocated with highest chlorophyll *a* (chl *a*) concentrations near the surface (5-80 m depth; Fig.2c) (Loginova et al., 2016). The oxycline was located at upper 5-80 m depth, here oxygen concentrations dropped from >200 µmol kg^{-1} to <1µmol kg^{-1} (Fig.2d) (Thomsen et al., 2016a). In summary, our observations were carried out during a period which corresponds to typical summer conditions off Peru.

2.2 Discrete water sampling and analyses

Seawater was sampled with a GO rosette equipped with a conductivity, temperature and depth profiler (CTD; Sea-Bird (SBE) 9-plus, Sea-Bird Electronics Inc., USA), an O_2 optode (SBE43, Sea-Bird Electronics Inc., USA), a WETStar chl *a* fluorometer (WET Labs, USA) and 24 x 10 L Niskin bottles. Additional water samples were taken with a PUMP-CTD-System (an integrated measurement device, which was developed in collaboration between Leibniz-Institut für Ostseeforschung (IOW) and the Max-Planck-Institut für Marine Mikrobiologie (MPI) Bremen: PUMP-CTD; Strady et al., 2008). In general, samples were collected at 3 to 8 sampling depths from 2 to 70 m at the onshore stations (~10km offshore) and from 2 to 200 m at stations offshore (~100 km offshore). DOC/DON analyses were performed for 50 GO rosette stations, and for 8 PUMP-CTD stations. Dissolved combined (hydrolysable) AA (DHAA) and dissolved combined CHO (DCCHO) analyses were performed only for samples from the GO rosette. CTD, O_2 and chl *a* recordings were taken at 172 profiles (Fig.1a).

The CTD was calibrated with discrete seawater samples measured with a Guildline Autosal 8 model 8400B salinometer. The O_2 optode was calibrated by a combination of Winkler titration (Winkler, 1888; Hansen, 1999) and STOX sensor measurements (Revsbech et al., 2009). Salinity and O_2 measurements had precision of 0.002 g kg^{-1} and ~ 1 µmol kg^{-1}, respectively. More details on the salinity and O_2 calibrations can be found in Thomsen et al. (2016a). Apparent oxygen utilization (AOU) was then calculated as a difference of measured O_2 concentrations and its equilibrium saturation using Gibbs-Sea Water Oceanographic Toolbox (McDougall and Barker, 2011) for MatLab (MathWorks, USA) for analyses of potential relationship between DOM reworking and the utilization of O_2.

The original fluorometer calibration provided by the sensor manufacturer (WET Labs, USA) was used throughout the cruise resulting in chl *a* concentrations in µg L^{-1}. More detail on the recalibration of the chl *a* fluorimeter one can find in Loginova et al. (2016).

Net primary production (NPP) was estimated for study area off Peru (12°S-14°S and 76°W-79°W) and the corresponding time period (February 2013) after the model of Behrenfeld and Falkowski (1997a) with Ocean Productivity toolbox (Oregon State University).

DOC/DON duplicate samples (20 mL) were collected into combusted glass ampoules (8 h, 450° C) after filtration with combusted GF/F filters (5 h, 450°C). Samples were acidified (80mL of 85% H_3PO_4), sealed with flame and stored at 4°C in the dark until analysis. DOC samples were analysed by the high-temperature catalytic oxidation method (TOC -VCSH, Shimadzu) modified from Sugimura and Suzuki (1988). The detection limit (DL) was 1µmol L^{-1}. Total dissolved nitrogen (TDN) was determined simultaneously to DOC with DL of 2 µmol L^{-1} using the TNM-1 detector of a Shimadzu analyser [Dickson et al., 2007]. DON concentrations were calculated by subtracting inorganic nitrogen concentrations from concentrations of TDN. The description of the instrument calibration and measurements may be found in Loginova et al. (2015).

Duplicate samples (~16ml) for DCCHO were collected into combusted (8hrs, 450°C) 25ml-glass vials after passing through 0.45 µm syringe filters (GHP membrane, Acrodisk, Pall Corporation) and immediately frozen at -20°C until analyses. Analyses were conducted by high performance anion exchange chromatography (HPAEC) coupled with pulsed amperometric detection following Engel and Händel (2011). Prior to analyses samples were thawed at room temperature and desalinated by membrane dialysis (1 kDa MWCO, Spectra Por, 5 h at 1°C). Desalinated duplicate subsamples (2 mL) were hydrolyzed using 1.6mL of 1M HCl (for each) for 20 h at 100°C. The hydrolyzed samples were neutralized through acid evaporation under N_2 atmosphere and an addition of miliQ water (20mL). DCCHO monomers were determined from 17.5 mL subsamples on a Dionex ICS 3000 system. More detailed method and calibration descriptions are given in Engel and Händel (2011). The method DL was ~10 nmol L^{-1} and precision of 2%. During our study, three classes of polysaccharides were measured. Those are neutral (fucose (Fuc), rhamnose (Rha), arabinose (Ara), galactose (Gal), glucose (Glc), mannose (Man) and xylose (Xyl)), amino (glucosamine (Glc-N) and galactosamine (Gal-N)), and the acidic sugars including gluconic acid (Glu-H)) and the uronic acids (DURA) galacturonic acid (Gal-URA) and glucuronic acid (Glc-URA). Man and Xyl were quantified as a mixture due to co-elution, and, therefore, reported together (ManXyl). Concentrations of DCCHO after hydrolysis are given as monomer equivalents.

Duplicate samples (~3ml) for DHAA were filtered with 0.45 µm syringe filters (GHP membrane, Acrodisk, Pall Corporation) and stored frozen (-20°C) in combusted (8hrs, 450°C) 4ml-glass vials until analyses. Samples were thawed and hydrolyzed with 6 N HCl at 100°C for 20 h prior to analysis. DHAA were determined by HPLC after ortho-phthaldialdehyde derivatization (Lindroth and Mopper , 1979; Dittmar et al., 2009) with DL of 2 nmol L^{-1} and precision of <5%. The following amino acids were analyzed during the study: α-amino acids: aspartic acid (Asp), glutamic acid (Glu), serine (Ser), arginine (Arg), glycine (Gly), threonine (Thr), alanine (Ala), tyrosine (Tyr), valine (Val), phenylalanine (Phe), isoleucine (Ileu), leucine (Leu) and γ-amino acid: γ-aminobutyric acid (GABA). Alpha amino butyric acid was used as an internal standard to account for losses during handling. Concentrations of DHAA

after hydrolysis are given as monomer equivalents. More in-detail description of the method may be found in (Engel and Galgani, 2016).

2.3 Diapycnal flux calculations

To estimate the diapycnal fluxes of various solutes, CTD sensor (O_2) and bottle data (DOC, DON, DCCHO and DHAA) were combined with near-simultaneous measurements of turbulence in the water column. The turbulence measurements were performed with a microstructure profiling system (MSS) from the rear of the vessel. The loosely-tethered profiler (MSS90-D, S/N 32, Sea &Sun Technology) was optimized to sink at a rate of 0.55 m s^{-1} and was equipped with three shear sensors and a fast-response temperature recorder, as well as an acceleration sensor, two tilt sensors and CTD, sampling with lower response time. At each CTD station, 3-6 microstructure profiles were collected. Standard processing procedures were used to determine the rate of kinetic energy dissipation of turbulence in the water column (ε in m^2s^{-3}), as given in Schafstall et al. (2010).

Diapycnal diffusivities (K_ρ in m^2s^{-1}) were determined following Osborn (1980):

$$K_\rho = \Gamma \frac{\varepsilon}{N^2}, \quad (1)$$

where N is stratification (in s^{-1}) and Γ is the mixing efficiency, for a which value of 0.2 was used. The diapycnal diffusivity of the solutes (O_2, DOC, DON, DCCHO, and DHAA) - K_S – was assumed to be equivalent to the diapycnal diffusivity of the mass K_ρ (e.g. Schafstall et al., 2010; Fischer et al., 2013).

The diapycnal fluxes (in mol m^{-2} s^{-1}) of the different solutes listed above were estimated using Eq.2, implicitly assuming equivalency of vertical and diapycnal diffusivities ($K_s \approx K_\rho$).

$$\Phi_S = -K_\rho \nabla C_S, \quad (2)$$

where ∇C_S is the vertical gradient of the molar concentration of the solutes (in mol m^{-4}).

Here, we define the diapycnal supply (in mol m^{-3} s^{-1}) of a solute as its vertical flux divergence, i.e. the change of the diapycnal flux with depth:

$$-\overline{\nabla \Phi_s} = -\frac{\partial}{\partial z}\overline{\Phi_S}, \quad (3)$$

For DCCHO and DHAA the diapycnal flux estimates were based on 14 combined CTD/MSS stations, while for DOC and DON fluxes 22 stations were available (Fig.1b). The diapycnal O_2 flux was determined from 50 combined stations. All combined data sets include stations from the continental slope, as well as stations in deeper waters, where bottom depth was larger than 4000m.

For each combined CTD/MSS station a mean K_ρ was estimated based on a N^2 profile (CTD) and mean dissipation profile (turbulence probe) averaged over all MSS profiles conducted at the CTD station. In combination with the vertical solute gradient a mean flux profile for each station was estimated. Only measurements below the mixed layer, which was defined by a threshold criterion of 0.2°C temperature decrease below the maximum and a minimum depth of 10 m, were used. Measurements from different sensors and instruments were combined in temperature space to reduce the impact of internal waves.

Biogeosciences Discuss., https://doi.org/10.5194/bg-2018-284
Manuscript under review for journal Biogeosciences
Discussion started: 15 June 2018

The mean diapycnal flux ($\overline{\Phi}_S$) was determined by arithmetically averaging all fluxes from individual stations in 14m depth intervals. The diapycnal solute supply was then determined from the divergence of the mean diapycnal flux ($\overline{\nabla\Phi}_S$).

The 95% confidence interval of the diapycnal flux was calculated following the procedure described by Schafstall et al. (2010). From this error estimate the uncertainty of the supply was derived by error propagation.

A simple equation of carbon combustion:

$$1C + 1O_2 = 1CO_2, \quad (4)$$

was used for a rough estimation of the percentage of diapycnal O_2 supply, that may be consumed by heterotrophic communities, if they use all the C, supplied by the diapycnal fluxes of DOC, DCCHO and DHAA.

2.4 Statistical analyses of DOM composition

Principal component analysis (PCA) was performed using environmental factors (temperature, salinity and AOU) and relative abundances of α-DHAA and neutral DCCHO (mol%) to examine "compositional trends" (i.e. changes in composition in response to an influence of an environmental parameter) in marine DOM in the studied area. The aim of the PCA was also to explore the potential interrelation between low-O_2 and DOM composition. For this, temperature, salinity and AOU and relative abundances of labile organic matter from open Atlantic and Pacific Oceans (Kaiser and Benner, 2009) were included in the PCA for the representation of well oxygenated water column. The covariance between principle components and an individual parameter was considered significant, when module of the coordinate of the parameter exceeded 0.5 on the "variables factor map". The PCA was performed using "FactorMineR" package (Husson et al., 2010) for "R" (R Core Team, 2013).

3 Results

3.1 Distribution of O_2 and DOM

In this section the horizontal and vertical distribution of O_2 and the different DOM components including DOC, DON and their labile and semi-labile constituents, DCCHO and DHAA are described. The vertical gradients of the different solutes are crucial for estimating the associated diapycnal fluxes, as described in section 3.2. Near surface O_2 concentrations were observed ranging between 100 µmol kg^{-1} at the coast and 240 µmol kg^{-1} further offshore (Fig. 2d). These values dropped to below 1 µmol kg^{-1} at ~80 m depth (Fig. 2d). DOC concentrations ranged from more than 100 µmol L^{-1} near the surface to < 50 µmol L^{-1} below 40 m depth (Fig.3a). Patches of isolated DOC maxima (up to 120 µmol L^{-1}) were measured at a depth range from 20 to 120 m (Fig.3a). Beside those isolated DOC maxima, the main decrease of DOC occurred at a depth range between 5 and 30 m. Thus, the main vertical DOC gradient was found at shallower depth, compared to the oxycline. This becomes visible, when comparing the mean vertical profiles of O_2 and DOC (Fig.4a,b).

DON concentrations were also highest (~7-8 µmol L^{-1}) near the surface (Fig.3b) and varied from below the detection limit to 4-5 µmol L^{-1} at greater depth. The main decrease of the DON concentrations occurred in the upper 10 m of

the water column (Fig.4c). The differences of the DON concentrations at greater depth were not high enough to obtain a significant gradient.

DCCHO concentrations varied from 0.2 µmol L^{-1} to 4.2 µmol L^{-1} (Fig.3c), with highest concentrations near the surface. C contained in DCCHO represented from 1 to 25 % of DOC in the studied depth range. Amino-sugars and DURA and Glc-H comprised 0.04±0.03 µmol L^{-1} and 0.02±0.02 µmol L^{-1}, that contributed 6±3 % and 3±2 % to DCCHO, respectively, leaving the major part of DCCHO to neutral sugars. DHAA concentrations varied from 0.075 µmol L^{-1} to 1.39 µmol L^{-1} (Fig.3d). Like for DCCHO, the highest DHAA concentrations were found above the oxycline, where C contained in DHAA represented up to 4 %DOC and nitrogen (N) contained in DHAA represented up to 82 % DON. Lowest DHAA concentrations were mainly found below 80 m depth and equivalent to ~1 %DOC and ~1 %DON. Similar to DOC, DCCHO and DHAA concentrations decreased in the upper part of the oxycline (Fig.4a,d,e,f). In summary, the concentrations of all the DOM compounds were highest above the oxycline, and the mean concentration gradients of the DOM compounds were restricted to a shallower depth, compared to the mean gradient of O_2.

3.2 Diapycnal fluxes and supply

As outlined in the previous section steep vertical gradients of O_2, DOC, DON and their constituents were observed at 30 to 80 m depth in the study area. In this section we combine these vertical gradients with turbulence measurements to estimate the associated diapycnal fluxes and supply i.e. the diapycnal flux divergences.

For O_2, the mean diapycnal flux ($\overline{\nabla\Phi}_{O2}$) exhibited a maximum of 50 mmolO_2 m^{-2} day^{-1} at ~20m depth. It deceased over the depth and vanished at 80m depth due to lack of vertical concentration gradients. The mean diapycnal supply O_2 ($\overline{\nabla\Phi}_{O2}$), ranged from 1.2 µmol kg^{-1} day^{-1} at 10-24 m depth to zero at 80 m depth.

In contrary, mean diapycnal fluxes of DOC ($\overline{\Phi}_{DOC}$) was limited to shallower depth. Near the surface, $\overline{\Phi}_{DOC}$ was 31 mmolC m^{-2} day^{-1} and vanished already at ~50 m depth (Table 2). Compared to NPP, estimated to 3.9 (0.6-8.6) gC m^{-2} day^{-1} for our study area and period, the DOC flux represented from a maximum of ~10(4-62) %NPP at ~20 m depth to near zero %NPP at ~50 m depth. The diapycnal supply of DOC ($\overline{\nabla\Phi}_{DOC}$) exhibited a maximum of 1.8 µmolC $kg^{-1}$$day^{-1}$ at 10-38 m depth (1.5 times larger than$\overline{\nabla\Phi}_{O2}$.) (Table 2, Eq. 4). As it was mentioned in the section 3.1, we did not find a significant vertical DON gradient, resulting in very low diapycnal DON fluxes and supply estimates (Table 2). However, significant N fluxes were obtained from DHAA transport. Mean C and N fluxes via DCCHO and DHAA ranged from near zero below 30-40 m depth to 6 mmolC m^{-2} day^{-1} ($\overline{\Phi}_{DCCHO(C)}$), 0.9 mmolC m^{-2} day^{-1} ($\overline{\Phi}_{DHAA(C)}$)and 0.1mmolN m^{-2} day^{-1} ($\overline{\Phi}_{DHAA(N)}$) at 10-20m depth (Table 2). The diapycnal C and N supply via DCCHO and DHAA ranged from near zero to a maximum of 0.4 µmolC $kg^{-1}day^{-1}$ ($\overline{\nabla\Phi}_{DCCHO(C)}$), 0.06 µmolC $kg^{-1}day^{-1}$($\overline{\nabla\Phi}_{DHAA(C)}$), and 0.02 µmolN $kg^{-1}day^{-1}$($\overline{\nabla\Phi}_{DHAA(N)}$) at 10-38 m depth. The diapycnal C supply via DCCHO and DHAA at its maximum comprised ~38% of $\overline{\nabla\Phi}_{O2}$, when estimated by Eq. (4). In summary, our diapycnal flux and supply calculation revealed that the diapycnal O_2 supply reaches deeper into the oxycline than the diapycnal DOM supply. This is especially true for DCCHO and DHAA, representing the labile and semi-labile parts of DOM.

3.3 Linking the DOM composition and the utilization of O_2

Biogeosciences Discuss., https://doi.org/10.5194/bg-2018-284
Manuscript under review for journal Biogeosciences
Discussion started: 15 June 2018

To understand, whether low-O_2 conditions of the OMZ may cause changes in DOM composition, we complement our quantitative estimates of the DOM and O_2 supply with the analyses of DOM quality. For this, the composition of neutral DCCHO and DHAA via PCA was compared to environmental factors, i.e. temperature, AOU and salinity, and to OM composition from the well oxygenated water column as described in Kaiser and Benner (2009). The first principle component (Dim 1) (Fig.5, "variables factor map") of the PCA was strongly influenced by AOU, indicating the interrelation of the DOM composition and removal of O_2. The utilization of O_2 was accompanied by selective removal of Glu, Phe, Leu, ILeu and Ser, and Rha, Gal, and Fuc (Fig.5, Table 1). Gly, Thr and Clc mol% were increasing along with increase in AOU (Fig.5). In general, the composition of DOM from the surface samples from our study was similar to the composition of DOM from the samples, collected from well oxygenated open ocean sites by Kaiser and Benner (2009), as the individual scores of the samples cluster together on Dim.1 of the PCA (Fig.5, "individuals factor map"). The samples, collected within the OMZ were much poorer in composition, even in comparison to the deepest open ocean samples (~4000m), as they grouped from the negative side of Dim. 1.

The differences on the second dimension of PCA (Dim.2) were driven likely by regional differences in the DOM composition, i.e. by mol% of Ala, Arb, and Fuc, and distributions of mol% Asp, Phe, Val and Leu over depth (Fig.5, Table 1, Kaiser and Benner, 2009).

4 Discussion

The observed distributions of O_2 as well as the DOC and DON components are the result of sinks and sources in the water column due to biogeochemical processes and isopycnal and diapycnal supply (i.e. flux divergences) controlled by physical processes. Previous studies have shown that turbulent mixing processes in the eastern boundary upwelling regions are strongly enhanced and that the resulting diapycnal supply is often a leading term in the flux divergence balances of O_2, nutrients and other solutes in the upper ocean (e.g. Schafstall et al., 2010; Kock et al., 2012; Brandt et al., 2015; Steinfeldt et al., 2015). The diapycnal O_2 and DOM fluxes and supply determined in this study represents an average value for the continental margin ranging from the shelf to about 100km offshore. The spatial averaging is likely responsible for lower near-surface diapycnal O_2 flux (50 $mmolO_2\ m^{-2}\ day^{-1}$) from our study compared to diapycnal O_2 fluxes determined in the Mauritanian upwelling, although vertical gradients of O_2 are much reduced in the latter upwelling system. There, a near-surface diapycnal O_2 flux of 73 $mmolO_2\ m^{-2}\ day^{-1}$ was determined during the high productivity season in boreal winter (Brandt et al., 2015). In their study, the diapycnal O_2 flux was able to sustain benthic O_2 uptake on the continental shelf up to a bottom depth of 100m. Rates of oxygen consumption in the upper-ocean from *in situ* incubations in the ETSP off Peru found values of about 1 $\mu mol\ kg^{-1}\ day^{-1}$ at depth of 50-80m during the Austral summer season (Kalvelage et al., 2015), which are comparable to similar estimates for North and South Pacific OMZs from Revsbech et al. (2009) and Tiano et al. (2014). The diapycnal O_2 supply estimated in this study is of similar magnitude and highlights the important role of turbulent processes for the O_2 ventilation of the upper oxycline off Peru. Other mixing terms of the O_2 transport budget, such as isopycnal O_2 supply by meso- (Thomsen et al., 2016a) and submesoscale (Thomsen et al., 2016b) dynamics or O_2 fluxes due to upwelling (e.g. Steinfeldt et al., 2015) may provide an additional loss of O_2 to the upper ocean, particularly in the region of the continental slope and the shelf. Furthermore, seasonal variations of the diapycnal solute fluxes may

occur due to, for instance, deepening the mixed layer during winter season (Echevin et al., 2008). Therefore, our results should be considered as the first estimates of diapycnal fluxes and supply in ETSP off Peru during austral summer. Therefore, more observations shall improve the robustness of the flux estimates.

DOM transport through the water column is restricted to advective and diffusive mixing processes. However, DOM is affected also by other abiotic or biological processes in the water column. For instance, the observed very low diapycnal DON flux may suggest a DON removal in the upper water column. Low concentrations of inorganic nutrients above 20 m depth (Thomsen et al., 2016a), and an overall nitrogen limitation that was found to be characteristic for the surface communities in the ETSP off Peru (Franz et al., 2012b), might force those communities to switch to organic nitrogen sources (e.g. Bradley et al., 2010), therefore reducing DON in the upper water column. Photoreactions could also reduce DON incorporated into large chromophoric molecules through production of volatile N compounds or inorganic N (Zepp et al., 1998). Thus, DOM composition was suggested to be affected by the photochemistry in our study area (Galgani and Engel, 2016, Loginova et al., 2016). Photochemical degradation to CO, CO_2 and other volatile compounds (Zepp et al., 1998) could lower the near surface diapycnal DOC flux, as well. Herewith, in our study, the diapycnal DOC flux was in the same order of magnitude as the diapycnal O_2 flux in the upper 20 m of the water column. An annual diapycnal DOC flux (4±7 molC $m^{-2}yr^{-1}$), estimated from our results by averaging of $\overline{\Phi}_{DOC}$ over the upper 50 m water depth and integrating over a year, is in the same order of magnitude as previously reported data for the North Pacific Subtropical Gyre, where DOC export was estimated by a mass balance approach (1.6-2.7 molC m^{-2} yr^{-1}; Emerson et al., 1997) and by fitting an exponential decay function over depth (0.5±0.1 molC m^{-2} yr^{-1}; Kaiser and Benner 2012). The diapycnal DOC flux represented a significant fraction of NPP (~10%NPP), and was comparable to the POC export, reported for the ETSP off Chile (~12 %NPP at 30m depth; Pantoja et al., 2004), and for the ETSP off Peru (~6 %NPP at 52m; Gagosian et al., 1983; 16-42% NPP near the surface; Kalvelage et al., 2013), advocating turbulent mixing of DOM to be an important C export mechanism in the upper oxycline. The diapycnal DOC supply was stronger, than the diapycnal O_2 supply, suggesting that DOM could potentially deliver more than enough organic material for O_2 to be respired in the upper water column. The vanishing of DOC flux above the upper oxycline may indicate that the bioavailable fraction of DOM is consumed well before entering the OMZ. This is even more apparent, when considering diapycnal DHAA and DCCHO fluxes, which decay more rapidly compared to the diapycnal DOC flux, suggesting their preferential uptake in the water column. The diapycnal supply of DHAA and DCCHO cannot fully explain the diapycnal supply of DOC, as those were responsible for only ~26% of $\overline{\nabla\Phi}_{DOC}$ when summed up together. This may hint to a presence of an additional bioavailable DOM component that is respired in the water column, and/or to other DOM removal mechanisms in the near-surface waters. For instance, DOM may form marine microgels and hence POM (Chin et al., 1998; Engel et al., 2004, Verdugo et al., 2004) or be trapped in the pore space of already existing particles (e.g. Benner, 2002).

A strong reworking of the labile and semi-labile DOM could also be seen from the analyses of DHAA and DCCHO composition. For instance, Glc was previously suggested to be less susceptible to microbial degradation compared to preferentially removed Fuc, Gal, and Ara (Ittekot et al., 1981; Sempere et al., 2008; Goldberg et al., 2010; Engel et al., 2012). Enrichment in Gly with depth was also previously proposed to be reflection of low nutritional value of Gly for organisms in anoxic sediments in ETSP off Chile (Pantoja and Lee, 2003) and in sediments of the North Sea (Dauwe and Middelburg, 1998). In our study, DHAA and DCCHO below 50 m depth were mainly composed by Gly

and Glc, respectively, indicating a significant stage of DOM reworking. Despite the shallow depth, DOM below 50 m depth was characterized by much stronger alteration than samples collected by Kaiser and Benner (2009) from much greater depths (up to 4000m), suggesting a rapid and extensive heterotrophic DOM utilization in ETSP. This rapid utilization of DOM could prevent labile and semi-labile DOM export into the OMZ, and also implies pronounced heterotrophic respiration, as DOM composition was highly interrelated to AOU. Herewith, the diapycnal supply of DHAA and DCCHO may explain up to 38% of $\overline{\nabla\Phi}_{O2}$. This suggests that the utilization of labile and semi-labile DOM is an important controlling factor of the shape of the upper oxycline of the OMZ, while the attenuation of O_2 in deeper parts of the upper water column is likely to be explained by other bioavailable OM sources, such as POM.

5 Conclusions

Our results suggest that DOM, i.e. DCCHO and DHAA, is significantly consumed and altered above the upper oxycline in the ETSP off Peru. Thus, despite the presence of high DOC concentrations in the euphotic zone, DOM may enter the OMZ in an already highly reworked stage. Herewith, DOM respiration may contribute substantially (~38%) to O_2 reduction in the upper water column, potentially controlling the shape of the upper oxycline of the OMZ. The elevated diapycnal supply of DOC to the upper oxycline, which cannot be explained by microbial processes solely, hint to the presence of additional DOM removal mechanisms, such as microgel formation or absorption onto particles.

6 Data availability

The microstructure profiles are available at https:/doi.org/10.1594/PANGAEA.868400. The O_2, temperature, salinity and nutrients were published at https:/doi.org/10.1594/PANGAEA.860727. The DOM data will be available at PANGAEA after publication.

7 Competing interests

The authors of this manuscript are not aware of any real or perceived financial conflicts of interests for other authors or authors that may be perceived as having a conflict of interest with respect to the results of this paper.

8 Acknowledgments

This study was supported by the Deutsche Forschungsgemeinschaft (dfg.de) trough SFB754 “Climate-Biogeochemical Interactions in the Tropical Ocean” (subproject B9) and CP1403 “Transfer and remineralization of biogenic elements in the tropical oxygen minimum zones”.

We thank the chief scientists of the M93 cruise G. Lavik and T. Kanzow for station planning and support during sampling, as well as the crew and scientists onboard. We are also grateful to G. Krahmann for processing the CTD

data, to C. Mages and R. Flerus for help with the water sampling, to J. Roa and R. Flerus for technicial support. Special thanks to F.Le Moigne for help with NPP estimations.

References

Amon, R.M.W., Fitznar, H.P., and Benner, R.: Linkages among the bioreactivity, chemical composition, and diagenetic state of marine dissolved organic matter, Limnol.Oceanogr., 46(2), 287-297, doi:10.4319/lo.200146.2.0287, 2001.

Arísteguí, J., Duarte, C.M., Agustí, S., Doval, M., Álvarez-Salgado, X.A., and Hansell, D.A.: Dissolved Organic Carbon Support of Respiration in the Dark Ocean, Science, 298, 1967, 2002.

Behrenfeld, M.J. and Falkowski. P.G.: Photosynthetic rates derived from satellite-based chlorophyll concentration, Linmol. Oceanogr, 42(1): 1-20, doi:10.4319/lo.1997.42.1.0001, 1997a.

Bender, M.L., and Heggie, D.T.: Fate of organic carbon reaching the deep sea floor: a status report, Geoch.Cosmoch.Asta, 48, 977-986, 1984.

Benner, R.: Chemical composition and reactivity, p.59–90. In D. A. Hansell and C. A. Carlson (eds), Biogeochemistry of Marine Dissolved Organic Matter. Academic Press, 2002.

Benner, R. and Kaiser, K.: Abundance of amino sugars and Peptidoglycan in marine particulate and dissolved organic matter, Limnol.Oceanogr., 48(1), 118-128, 2003.

Bradley, P.B., Sanderson, M.P., Frischer, M.E., Brofft, J., Booth, M.G., Kerkhof, L.J., and Bronk, D.A.: Inorganic and organic nitrogen uptake by phytoplankton and heterotrophic bacteria in the stratified Mid-Atlantic Bight, Est. Coast. And Shelf Sci, 88, 429-441, 2010.

Brandt, P., Bange, H.W., Banyte, D., Dengler, M., Didwischus S./H., Fischer, T., Greatbatch, R.J., Hahn, J., Kanzow, T., Karstensen, J., Körzinger, A., Krahmann, G., Schmidtko,S., Tanhua, T., and Visbeck, M.: On the role of circulation and mixing in the ventilation of oxygen minimum zones with a focus on the eastern tropical North Atlantic, Biogeosc. 12, 489-512, 2015.

Carlson, C.A., Hansell, D.A., and Tamburini, C.: DOC Persistence and Its Fate after Export within the Ocean Interior, p.57-59. In N. Jiao and F. Azam (eds.), Microbial Carbon Pump, Science/AAAS, 2011.

Chin, W.-C., Ollerana, M.V., Verdugo P.: Spontaneous assembly of marine dissolved organic matterinto polymers gels, Nature, 391, 568-572, 1998.

Czeschel, R., Stramma, L., Schwarzkopf, F.U. Giese, B.S., Funk, A., and Karstensen, J.: Middeldepth circulation of the easterntropical South Pacific and its link to the oxygen minimum zone, JGR: Oceans, 116, C1015, doi:10.1029/2010jc006565, 2011.

Dauwe, B. and Middelburg, J.J.: Amino acids and hexoamines as indicators of organic matter degradation state in North Sea sediments. Linmol. Oceanogr., 43(5), 782-798, 1998.

Davis, J., Kaiser, K., and Benner, R.: Amino acid and amino sugar yields and compositions as indicators of dissolved organic matter diagenesis, Org. Geochem., 40(3), 343-352, doi: 10.1016/j.orggeochem.2008.12.003, 2009.

Dickson, A. G., Sabine, C. L., and Christian, J. R.: Guide to best practices for ocean CO_2 measurements, PICES special publication 3, 2007.

Echevin, V., Aumont, O., Ledesma, J., and Flores, G.:The seasonal cycle of surface chlorophyll in the Peruvian upwelling system: A modelling study, Progr. Oceanogr., 79, 167-176, 2008.

Ekau, W., Auel., H., Pörtner, H.-O., and Gilbert, D.: Impact of hypoxia on the structure and processes in pelagic communities (zooplankton, macro-intervertebrates and fish), Biogeosc. 7,1669-1699, 2010.

Emerson, S., Quay, P., Karl, D., Winn, C., Tupas L., and Landry M.: Experimental determination of the organic carbon flux from open-ocean surface waters, Nature, 389, 951-954, doi:10.1038/40111, 1997.

Engel, A., Thoms, S., Riebesell, U., Rochelle-Newall, E., and Zondervan, I.: Polysaccharide aggregation as a potential sink of marine dissolved organic carbon, Nature, 428, 929-932, 2004.

Engel, A. and Galgani L.: The organic sea surface microlayer in the upwelling region off Peru and implications for air–sea exchange processes, Biogeosc., 13, 989-1007, doi:10.5194/bg-13-989-2016, 2016.

Engel, A., and Händel, N.: A novel protocol for determining the concentration and composition of sugars in particulat and in high molecular weight dissolved organic matter (HMW-DOM) in seawater, Mar. Chem., 127, 180-191, 2011.

Engel, A., Händel, N., Wohlers, J., Lunau, M., Grossart, H.P., Sommer, U., and Riebesell, U.: Effects of sea surface warming on the production and composition of dissolved organic matter during phytoplankton blooms: results from a mesocosm study, J. Plankt. Res., 33(3), 357-372, doi: 10.1093/plankt/fbq122, 2011.

Engel, A., Harlay, J., Piontek, J., and Chou, L.: Contribution of combined carbohydrates to dissolved and particulate organic carbon after the spring bloom in the northern Bay of Biskay (North-Eastern Atlantic Ocean), Cont. Shelf Res., 45, 42-53, doi:10.1016/j.csr.2012.05.016, 2012.

Fischer, T., Banyte, D., Brandt, P., Dengler, M., Krahmann. G., Tanhua, T., and Visbeck, M.: Diapycnal oxygen supply to the tropical North Atlantic oxygen minimum zone., Biogeosc., 10, 5079–5093, doi:10.5194/bg-10-5079-2013, 2013. Franz, J., Krahmann, G., Lavik, G., Grasse, P., Dittmar, T., and Riebesell, U.: Dynamics and stoichiometry of nutrients and phytoplankton in waters influenced by the oxygen minimum zone in the eastern tropical Pacific, Deep-Sea Res. Part I, 62, 20–31, 2012a.

Franz, J.M.S., Hauss, H., Sommer, U., Dittmar, T., and Riebesell, U.: Production, partitioning and stoichiometry of organic matter under variable nutrient supply during mesocosm experiments in the tropical Pacific and Atlantic Ocean, Biogeosc., 9, 4629-4643, doi:10.5194/bg-9-4629-2012, 2012b.

Gagosian, R.B., Nigrelli, G.E., and Volkman, J.K.: Vertical Transport and Transformation of Biogenic Organic Compounds from a Sediment Trap Experiment off the Coast of Peru, from Coastal Upwelling and Its Sediment Record, p. 241-272. In E. Suess and J. Thiede (eds.), Nato Conference Series, volume 10B, doi:10.1007/978-1-4615-6651-9_13, Springer US, 1983.

Galgani, L., and Engel., A.: Changes in optical characteristics of surface microlayers hint to photochemically and microbially meditated DOM turover in the upwelling region off the coast of Peru, Biogeosc. 13, 2453-2473, 2016.

Gilly, W.F., Beman, J.M., Litvin, S.Y., and Robinson, B.H.: Oceanographic and biological effects of shoaling of the oxygen minimum zone, Ann. Rev. Mar. Sci., 5, 393-420, 2013, doi:10.1146/annurev-marine-120710-100849.

Goldberg, S.J. Carlson, C.A., Bock, B., Nelson, N.B., and Siegel D.A.: Meridional variability in dissolved organic matter stocks and diagenetic state within the euphotic and mesopelagic zone of the North Atlantic subtropical gyre, Mar.Chem., 119, 9-21, 2010.

Hahn, J., Brandt, P., Greatbatch, R.J., Krahmann, G., and Körtzinger, A.: Oxygen variance and meridional oxygen supply in the Tropical North East Atlantic oxygen minimum zone, Clim. Dynam., 43, 2999–3024, 2014.

Hansen, H.P.: Determination of oxygen, p.75-90. In K. Grasshoff, K. Kremling and M. Ehrhardt (eds.), Methods of seawater analysis, Verlag Chemie3d ed, 1999.

Harvey, H.R., Tuttle, J.H. and Bell, J.T.:Kinetics of phytoplankton decay during stimulated sedimentation: Changes in biochemical composition and microbial activity under oxic and anoxic conditions, Geochim. Cosmochim. Asta, 59, 3367-3377, 1995.

Husson, F., Le, S., and Pagès, J.: Exploratory Multivariate Analysis by Example using R. Boca Raton: CRC Press, 2010.

Ittekot, V., Brockmann, U., Michaels, W., and Degens, E.T.: Dissolved free and combined carbohydrates during a phytoplankton bloom in the northern North Sea, Mar.Ecol.Progr.Ser., 4(3), 299-305, 1981.

Jackson, G.A. and Williams, P.M.: Importance of dissolved organic nitrogen and phosphorus to biological nutrient cycling, Deep-Sea Res II, 3, 223–235, 1985.

Kaiser, K. and Benner, R.: Biochemical composition and size distribution of organic matter at the Pacific and Atlantic time-series station,. Mar. Chem., 113, 63-77, doi:10.1016/j.marchem.2008.12.004, 2009.

Kalvelage, T., Lavik, G., Lam, P., Contreras, S., Arteaga, L., Löscher, C.R., Oschlies, A., Paulmier, A., and others: Nitrogen cycling driven by organic matter export in the south pacific oxygen minimum zone, Nature Geosci, 6(3), 228-234, 2013.

Kalvelage, T., Lavik, G., Jensen, M.M., Revsbech, N.P., Loescher, C., Schunck, H., Desai, D.K., Hauss, H., and others.: Aerobic microbial respiration in oceanic oxygen minimum zones. PLoS ONE, 10(7), e0133526, doi:10.1371/journal.pone.0133526, 2015

Karstensen, J., Stramma, L., and Visbeck, M.: Oxygen minimum zones in the eastern tropical Atlantic and Pacific oceans, Progr.Oceanogr. 77, 331–350, doi:10.1016/j.pocean.2007.05.009, 2008.

Kock, A., Schafstall, J., Dengler, M., Brandt, P., and Bange, H.W.: Sea-to-air and diapycnal nitrous oxide fluxes in the eastern tropical North Atlantic Ocean, Biogeosc., 9, 957-964, doi:10.5194/bg-9-957-2012, 2012.

Lee, C., Wakeham, S.G., and Hedges, J.I.: Composition and flux of particulate amino acid and chloropigments in equatorial Pacific seawater and sediments, Deep-Sea Res.I, 47, 1535-1568, 2000.

Lindroth, P., and Mopper, K.: High performance liquid chromatographic determination of subpicomole amounts of amino acids by precolumn fluorescence derivatization with *o*-phthaldialdehyde, Anal.Chem., 51, 1667-1674, 1979.

Letscher, R.T., Hansell, D.A., Carlson, C.A., Lumpkin, R., and Knapp, A.N.: Dissolved organic nitrogen dynamics in global surface ocean: distribution and fate, Glob. Biogeochem. Cycles, 27, 141-153, 2013.

Loginova, A. N., Borchard, C., Meyer, J., Hauss, H., Kiko, R., and Engel, A.: Effects of nitrate and phosphate supply on chromophoric and fluorescent dissolved organic matter in the Eastern Tropical North Atlantic: a mesocosm study, Biogeosc., 12, 6897-6914, doi:10.5194/bg-12-6897-2015, 2015.

Loginova, A.N., Thomsen, S., and Engel, A.: Chromophoric and fluorescent dissolved organic matter in and above the oxygen minimum zone off Peru, J. Geophys. Res. Oceans, 121(11), 7973-7990, doi:10.1002/2016JC011906, 2016.

Mahadevan, A.: Eddy effects on biogeochemistry, Nature, 506, 168-169, 2014.

McDougall, T.J., and Barker, P.M.: Getting started with TEOS and the Gibbs Seawater (GSW) Oceanographic Toolbox, 28pp., SCOR/IAPSO WG127, ISBN 978-0-646-55621-5, 2011.

Nguyen R.T., and Harvey H.R.: Protein and amino acid cycling during phytoplankton decomposition in oxic and anoxic waters. Org. Geochem., 27, 115-128, 1997.

Ogawa, H., Tanoue, E.: Dissolved Organic Matter in Oceanic Waters, J. Oceanogr., 59, 129-147, 2003

Osborn, T.R.: Estimates of the local rate of vertical diffusion from dissipation measurements, J. Phys. Oceanogr. 10(1), 83-89, 1980.

Pantoja, S. and Lee, C.: Amino acid remineralization and organic matter lability in Chilean coastal sediments, Org. Geochem., 34, 1047-1056, 2003.

Pantoja, S., Sepúlveda, J., and González, H.E.: Decomposition of sinking proteinaceous material during fall in the oxygen minimum zone off northern Chile, Deep-Sea Res.I, 51, 55-70, 2004.

Pantoja, S., Rossel, P., Castro, R., Cuevas, L.A., Daneri, G., and Córdova, C.: Microbial degradation rates of small peptides and amino acids in the oxygen minimum zone of Chilean coastal waters, Deep-Sea Res.II, 56, 1055-1062, 2009.

Pennington, J.T., Mahoney, K.L., Kuwahara, V.S., Kolber, D.D., Calienes, R., and Chavez, F.P.: Primary production in the eastern tropical pacific: A review, Progr. Oceanogr,. 69(2-4), 285-317, doi: 10.1016/j.pocean.2006.03.012, 2006.

R Core Team: R: A language and environment for statistical computing. R Foundation for Statistical Computing, Vienna, Austria, URL http://www.R-project.org/, 2013.

Redfield, A.C.: The biological control of chemical factors in the environment, Am. Sci., 46, 205-221, 1958.

Revsbech, N.P., Larsen, L.H., Gundersen, J., Dalsgaard, T., Ulloa, O., and Thamdrup, B.: Determination of ultra-low oxygen concentrations in oxygen minimum zones by the stox sensor, Limnol. Oceanogr., Methods 7(5), 371-381, doi:10.4319/lom.2009.7.371, 2009.

Romankevich, E.A. and Ljutsarev. S.V.: Dissolved organic carbon in the ocean, Mar. Chem., 30, 161-178, 1990.

Schafstall, J., Dengler, M., Brandt, P., and Bange, H. W.: Tidal induced mixing and diapycnal nutrient fluxes in the Mauritanian upwelling region, J. Geophys. Res., 115, C10014, doi:10.1029/2009JC005940, 2010.

Sempere, R., Tedetti, M., Panagiotopoulos, C., Charriere, B., and Van Wambeke, F.: Distribution and bacterial availability of dissolved neutral sugars in the South East Pacific, Biogeosc., 5, 1165–1173, 2008.

Skoog, S. and Benner, R.: Aldoses in various size fractions of marine organic matter: Implications for carbon cycling, Limnol. Oceanogr., 42, 1803-1813, 1997.

Steinfeldt R., Sültenfuß, J., Dengler, M., Fischer, T., and Rhein, M.: Coastal upwelling off Peru and Mauritania inferred from helium isotope disequilibrium, Biogeosc., 12, 7519-7533, 2015.

Strady, E., Pohl, C., Yakushev, E.V., Krüger, S., and Hennings, U.: PUMP-CTD-System for trace metal sampling with a high vertical resolution. A test in the Gotland Basin, Baltic Sea, Chemosphere, 70(7), 1309-1319, 2008.

Sugimura, Y. and Suzuki Y.: A high-temperature catalytic oxidation method for the determination of non-volatile dissolved organic carbon in seawater by direct injection of a liquid sample, Mar. Chem., 24, 105–131, 1988.

Thomsen, S., Kanzow, T., Krahmann, G., Greatbatch, R. J., Dengler, M., and Lavik, G.: The formation of a subsurface anticyclonic eddy in the Peru-Chile Undercurrent and its impact on the near-coastal salinity, oxygen and nutrient distributions, J. Geophys. Res. Oceans, 121, 476–501, doi:10.1002/2015JC010878, 2016(a).

Thomsen, S., Kanzow, T., Colas, F., Echevin, V., Krahmann, G., and Engel, A.: Do submesoscale frontal processes ventilate the oxygen minimum zone off Peru?, Geophys. Res. Letters, 43, 8133–8142, doi:10.1002/2016GL070548, 2016(b).

Tiano, L., Garcia-Robledo, E., Dalsgaard, T., Devol, A.H., Ward, B.B., Ulloa, O., Canfield, D.E., and Revsbech, N.P.: Oxygen distribution and aerobic respiration in the north and south eastern tropical Pacific oxygen minimum zones, Deep-Sea Res.I, 94, 173-183, 2014.

Verdugo, P., Alldredge, A.L., Azam, F., Kirchman, D.L., Passow, U., Santschi, P.H.: The oceanic gel phase: A bridge in the DOM-POM continuum. Marine Chemistry 92:67–85, 2004

Winkler, L.W.: Die Bestimmung des Wassers gelösten Sauerstoffes, Berichte der deutschen chemischen Gesellschaft, 21(2), 2843-2854, doi:10.1002/cber.188802102122, 1888.

Zepp, R.G, Callaghan, T.V., and Erickson, D.J.: Effects of enhanced solar ultraviolet radiation on biogeochemical cycles, UNEP, Environmental effects of ozone depletion: 1998 Assessment, United Nations Environment Programme, 205pp, ISBN 92-807-1724-3, 1998.

Biogeosciences Discuss., https://doi.org/10.5194/bg-2018-284
Manuscript under review for journal Biogeosciences
Discussion started: 15 June 2018

Biogeosciences Discussions Open Access EGU

Table 1: Relative composition (mol%) of dissolved hydrolysable amino acids (DHAA) and dissolved combined carbohydrates (DCCHO)) in the water column, "n.d." - not detectable.

Depth (m)	DHAA (µmol L^{-1})	mol% DHAA														
		Gly	GABA	Thr	Ala	Asp	Glu	Ser	Arg	Leu	Val	Ileu	Phe	Tyr		
10-24	0.6±0.3	22±3	0.3±0.2	9±1	11±1	17±1	15±3	10±2	2.3±0.3	4±1	3.0±0.4	2.5±0.6	2.4±0.4	1.8±0.4		
24-38	0.5±0.3	23±4	0.4±0.2	9±2	11±1	17±1	15±4	10±1	2.2±0.4	4±1	2.9±0.6	2.1±0.5	2.1±0.4	1.7±0.3		
38-52	0.4±0.2	24±4	0.4±0.1	9±1	11±1	17±1	14±2	9±1	2.2±0.5	4±1	2.9±0.6	2.3±0.7	2.3±0.5	1.9±0.5		
52-66	0.3±0.1	28±3	0.5±0.3	10±2	12±1	17±1	11±2	9±1	1.8±0.4	3±1	2.5±0.6	1.9±0.6	1.8±0.5	1.9±0.6		
66-80	0.19±0.05	29±5	0.6±0.4	10±2	12±1	16±1	11±2	9±1	1.8±0.4	2±2	2.3±0.7	1.7±0.6	1.8±0.4	1.7±0.4		
80-94	0.16±0.05	32±3	0.8±0.7	10±1	12±1	16±1	10±2	8±1	1.6±0.4	2±1	2.4±0.9	1.6±0.8	1.7±0.4	1.7±0.5		
94-108	0.14±0.06	33±3	0.7±0.3	10±2	12±1	15±2	10±2	8±2	1.6±0.4	2±1	2.3±0.7	1.6±0.9	1.7±0.4	2±1		
108-122	0.12±0.03	35±3	0.8±0.4	10±2	12±2	15±2	9±1	8±2	1.5±0.5	2±1	2±1	1.8±0.8	1.6±0.4	1.5±0.5		
	DCCHO (µmol L^{-1})	mol% DCCHO														
		Glc	ManXyl	Gal	Rhm	Fuc	Ara	Glc-N	Gal-N	Glc-H	Gal-URA	Glu-URA				
10-24	1.6±0.9	26±11	28±5	14±6	10±8	7±2	2±1	7±3	0.1±0.2	3±2	3±1	n.d.				
24-38	1.3±0.7	29±10	29±5	14±5	7±5	7±2	2±1	7±2	0.2±0.4	2±2	3±1	0.2±0.9				
38-52	0.9±0.3	30±10	32±6	12±4	5±3	7±2	2±1	7±2	0.2±0.2	2±2	3±1	0.2±0.9				
52-66	0.6±0.2	36±11	34±8	8±4	3±2	6±2	1±1	8±3	0.2±0.3	1±2	3±2	n.d.				
66-80	0.5±0.2	38±9	37±8	7±3	2±2	4±2	1±1	7±3	0.1±0.2	1±2	3±2	n.d.				
80-94	0.5±0.2	41±10	39±10	5±2	1±1	4±2	1±1	5±2	0.1±0.2	1±2	3±3	0.1±0.9				
94-108	0.4±0.2	45±11	38±10	4±2	1±1	3±1	1±1	5±2	0.1±0.1	1±3	2±2	n.d.				
108-122	0.4±0.2	46±10	39±10	3±1	0.5±0.7	3±1	1±2	4±2	0.1±0.1	1±3	2±3	n.d.				

Biogeosciences Discuss., https://doi.org/10.5194/bg-2018-284
Manuscript under review for journal Biogeosciences
Discussion started: 15 June 2018

Table 2: Diapycnal fluxes and supplies (in bold) of O_2 and DOM: DOC, DON, dissolved organic carbon in DCCHO and DHAA and dissolved organic nitrogen in DHAA; averaged fluxes and supplies. Errors are presented in the brackets.

	Depth	DOC	DON	DCCHO-C	DHAA-C	DHAA-N	O_2
Flux (mmol m^{-2} day^{-1})	10-24	**31** (25)	**-0.6** (0.4)	**6** (2)	**0.9** (0.4)	**0.3** (0.1)	**50** (14)
	24-38	**5** (17)	**8** (6)	**0.2** (0.1)	**0.07** (0.03)	**0.03** (0.01)	**32** (10)
	38-52	**0.4** (0.5)	**0.4** (0.9)	**0.12** (0.07)	**0.07** (0.03)	**0.03** (0.02)	**32** (9)
	52-66	**0.2** (0.2)	**0.5** (1.3)	**0.01** (0.01)	**0.05** (0.02)	**0.02** (0.01)	**17** (6)
	66-80	**0.6** (0.7)	**0.1** (0.3)	**0.12** (0.06)	**0.02** (0.01)	**0.7×10^{-2}** (0.4×10^{-2})	**8** (4)
	80-94	**-0.04** (0.35)	**-0.1×10^{-2}** (0.3×10^{-2})	**0.14** (0.07)	**0.01** (0.02)	**0.4×10^{-2}** (0.5×10^{-2})	**0.12** (0.07)
	94-108	**-0.2** (0.2)	**0.05** (0.04)	**0.09** (0.08)	**0.6×10^{-2}** (0.5×10^{-2})	**0.2×10^{-2}** (0.1×10^{-2})	**0.016** (0.7×10^{-2})
	108-122	**-0.2** (0.2)	**0.01** (0.08)	**-0.01** (0.01)	**0.2×10^{-3}**(0.3×10^{-3})	**0.1×10^{-3}** (0.2×10^{-3})	**0.02** (0.01)
Supply (µmol L^{-1} day^{-1})	10-38	**1.8** (2.1)	-	**0.4** (0.2)	**0.06** (0.03)	**0.02** (0.01)	**1.2** (1.2)
	24-52	**0.3** (1.2)	**0.6** (0.4)	**0.5×10^{-2}** (0.8×10^{-2})	**0.1×10^{-3}** (3.2×10^{-3})	**0.2×10^{-4}** (0.14×10^{-3})	**0.04** (0.93)
	38-66	**0.01** (0.04)	**-0.01** (0.1)	**0.8×10^{-2}** (0.5×10^{-2})	**0.1×10^{-2}** (0.3×10^{-2})	**0.1×10^{-2}** (0.1×10^{-2})	**1.0** (0.8)
	52-80	**-0.03** (0.05)	**0.03** (0.09)	**-0.8×10^{-2}** (0.5×10^{-2})	**0.2×10^{-2}** (0.2×10^{-2})	**0.7×10^{-3}** (0.6×10^{-3})	**0.7** (0.5)
	66-94	**0.05** (0.05)	**0.01** (0.02)	**-0.1×10^{-2}** (0.7×10^{-2})	**0.1×10^{-2}** (0.2×10^{-2})	**0.2×10^{-3}** (0.5×10^{-3})	**0.5** (0.3)
	80-108	**0.01** (0.03)	**-0.3×10^{-2}** (0.3×10^{-2})	**0.4×10^{-2}** (0.8×10^{-2})	**0.4×10^{-3}** (1.4×10^{-3})	**0.1×10^{-3}** (0.4×10^{-3})	**0.7×10^{-2}** (0.5×10^{-2})
	94-122	**0.4×10^{-2}** (0.017)	**0.2×10^{-2}** (0.6×10^{-2})	**0.7×10^{-2}** (0.6×10^{-2})	**0.4×10^{-3}** (0.3×10^{-3})	**0.1×10^{-3}** (0.1×10^{-3})	**-0.1×10^{-2}** (0.1×10^{-2})

Figure 1: Study area and station map. CTD stations, where CTD-probe and fluorimeter measurements were accomplished are marked as black dots (a,b). PUMP-CTD stations are depicted in pink diamonds (a). CTD and PUMP-CTD stations, where DOM sampling was performed are marked as green stars (a). Microstructure measurements, combined with oxygen profiles are marked as grey circles (b). Microstructure measurements, combined with dissolved organic matter (dissolved organic carbon (DOC), dissolved hydrolysable amino acids (DHAA) and dissolved combined carbohydrates (DCCHO)) measurements marked as green pentagrams (b). Extra microstructure measurements, combined with DOC measurements marked with violet pentagrams (b). Shaded colors represent chl *a* concentrations at upper 10 m depth (a) and oxygen concentrations at 15m depth (b). Spaces between data points were interpolated by using TriScatteredInterp function (MATLAB, MathWorks).

Figure 2: Mean vertical distribution of the temperature (a), salinity (b), (c) chlorophyll *a* (chl *a*) and (d) O_2. O_2 values below 1 µmol kg^{-1} are shaded in violet. The data from all transects and stations were averaged over intervals of 10 km on "Distance from the coast" axis and over 1 m on "Depth" axis. Isolines represent potential density, averaged over intervals of 10 km on "Distance from the coast" axis and over 1 m on "Depth" axis.

Figure 3: Dissolved organic carbon (DOC) (a), dissolved organic nitrogen (DON) (b), dissolved combined carbohydrates (DCCHO) (c) and dissolved hydrolysable amino acids (DHAA) (d) distributions over the water column. Data from all transects and stations were plotted against distance to coast (km). Space between data points was interpolated by using TriScatteredInterp function (MATLAB, MathWorks). Isolines represent potential density, averaged over intervals of 10 km on "Distance from the coast" axis and over 1 m on "Depth" axis.

Figure 4: Vertical distribution of O_2 (a), DOC (b), DON (c), DCCHO(C) (d), DHAA(C) (e), DHAA(C) (f). Black line and error bar represent median distribution and standard deviations of the data points (grey circles), respectively.

Figure 5: The PCA analysis output: variables (on the left) and individuals scores of samples (from the right). The samples, collected above 50m depth are marked with acronym "s", the ones, below 50m depth – with acronym "d". The samples, which are used for comparison are marked with acronyms "HOT" and "BATS", and represented well oxygenated samples, collected from open Pacific and open Atlantic Oceans, respectively (Kaiser and Benner, 2009).

Biogeosciences Discuss., https://doi.org/10.5194/bg-2018-284
Manuscript under review for journal Biogeosciences
Discussion started: 15 June 2018

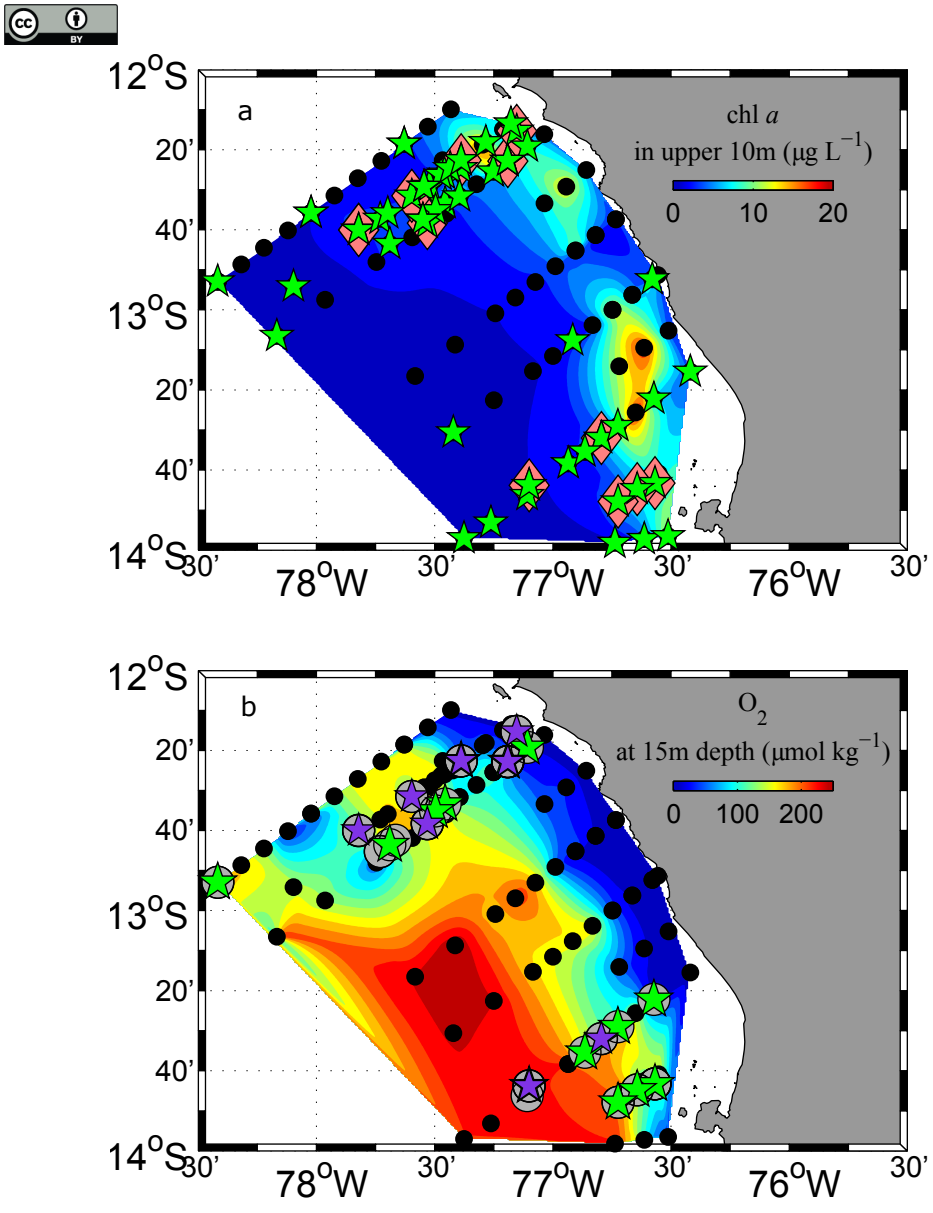

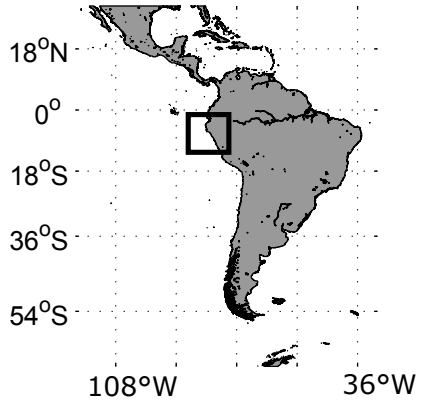

Biogeosciences Discuss., https://doi.org/10.5194/bg-2018-284
Manuscript under review for journal Biogeosciences
Discussion started: 15 June 2018

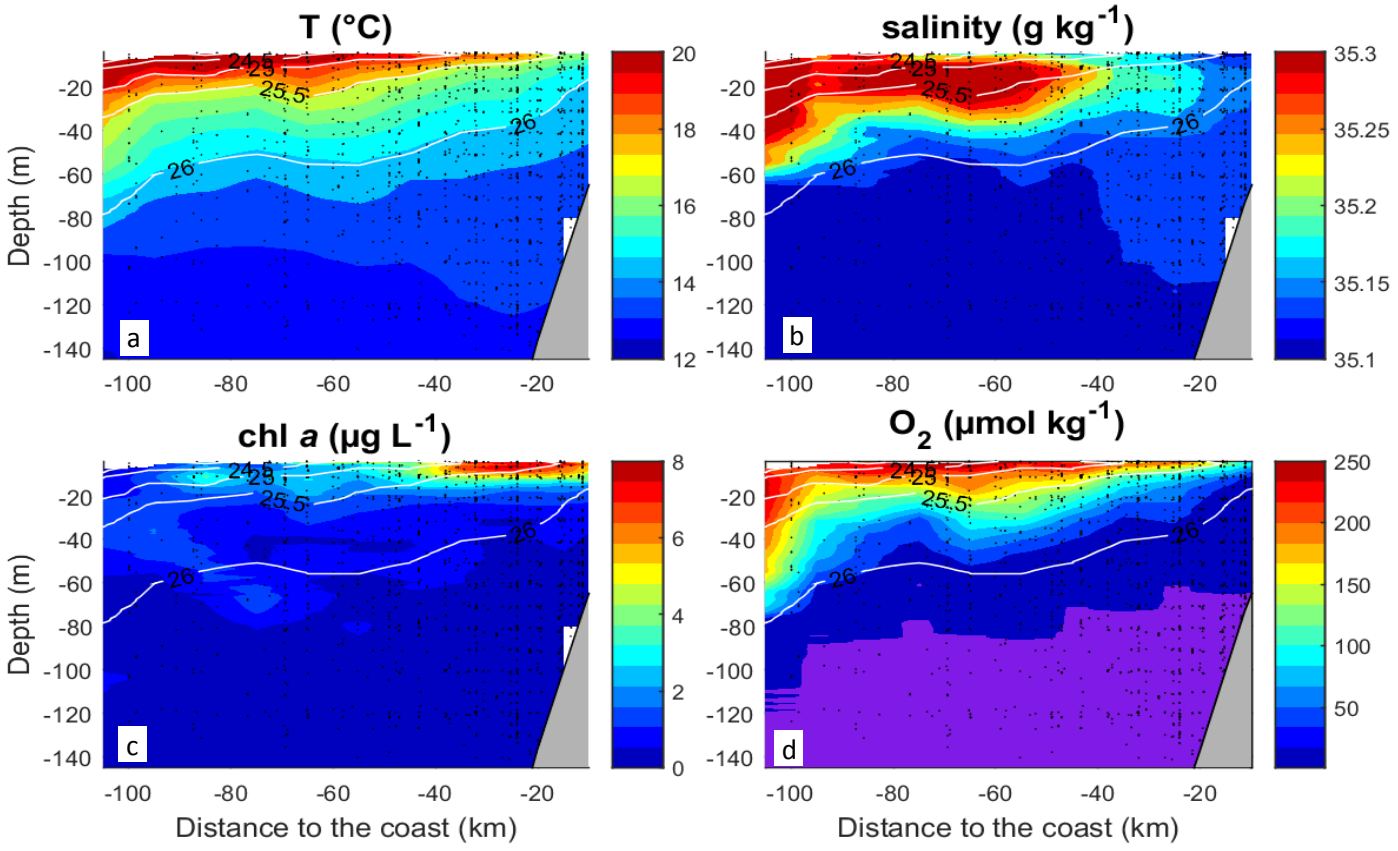

Biogeosciences Discuss., https://doi.org/10.5194/bg-2018-284
Manuscript under review for journal Biogeosciences
Discussion started: 15 June 2018

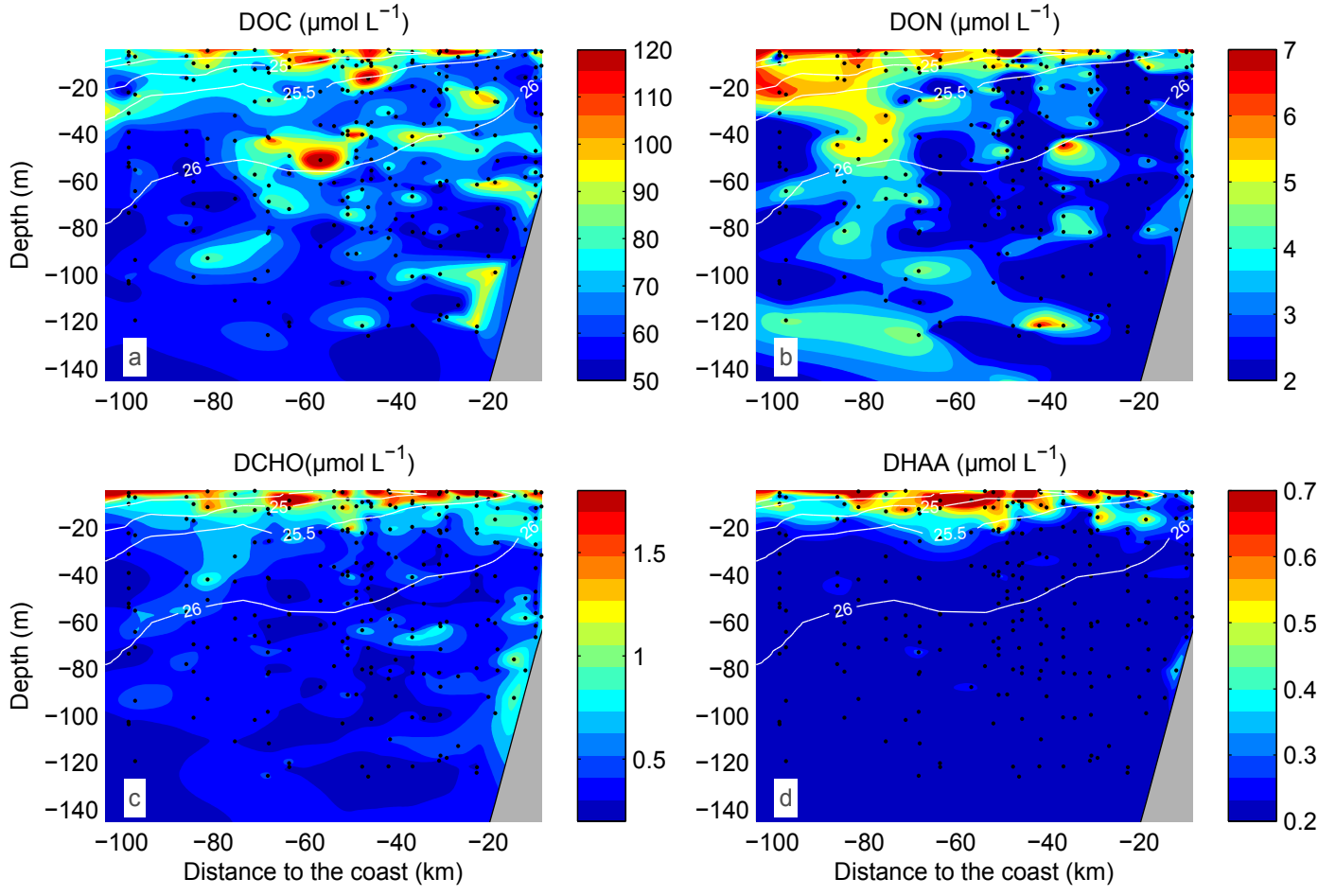

Biogeosciences Discuss., https://doi.org/10.5194/bg-2018-284
Manuscript under review for journal Biogeosciences
Discussion started: 15 June 2018

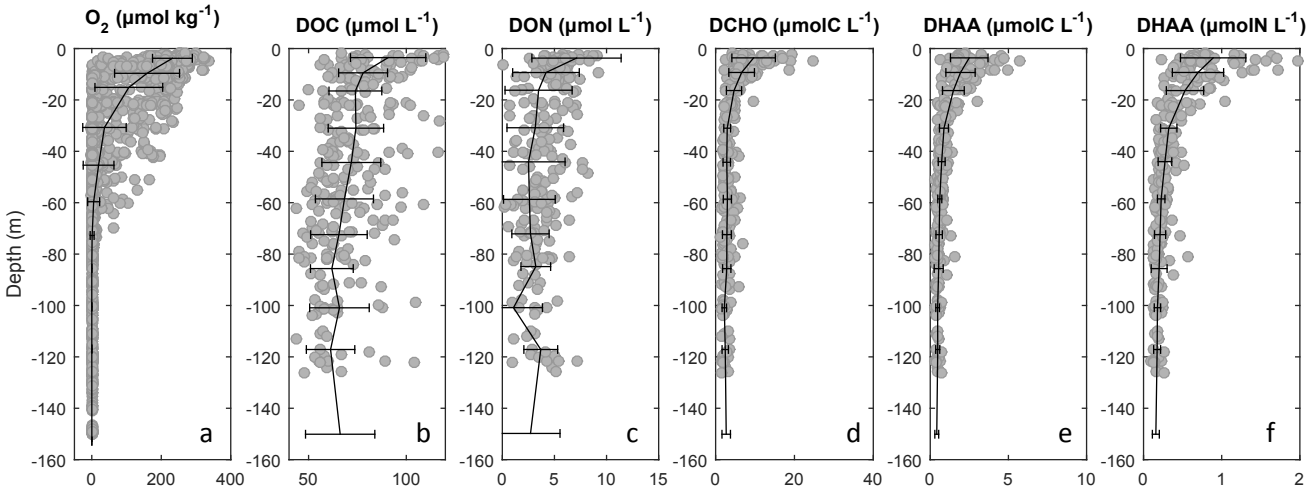

Biogeosciences Discuss., https://doi.org/10.5194/bg-2018-284
Manuscript under review for journal Biogeosciences
Discussion started: 15 June 2018